CRACK-TIP STRESS ANALYSIS FROM FIELD VALUES OF THE DISPLACEMENTS USING COMPLEMENTARY ENERGY

J. L. Swedlow[1], M. E. Karabin, Jr.[1] and G. E. Maddux[2]

A variety of techniques is now available for crack-tip stress analysis, and the need for further development along these lines may not at first be evident. For some circumstances, however, none of the present methods is especially applicable so that we have been moved to develop another approach. Concern here derives from having an experimental determination of displacements at points surrounding a crack's tip at the outset; the objective is to find the corresponding stress intensity factor(s). Such measurements are conveniently made at modest distances (a few cm) from the crack's tip; in the tip's immediate vicinity, however, experimental accuracy may be impeded by localized plastic flow, surface roughening, and dimpling. Objections to use of established analytical/numerical methods arise owing to indeterminacy of loads or overall structural complexity. We seek therefore to determine stress intensity factor(s) from *in situ* displacement data at points along a path or surface that surrounds the crack's tip but interior to the structure in which the crack is found.

To this end, *in situ* displacement data are taken to pertain to the difference between two excitation levels, one nominally at rest and the other at load. This pairing is required by whatever experimental method is employed; the analysis proceeds in terms of the net difference and gives either increment(s) in stress intensity factor(s) or total value(s) where the at-rest state is wholly unloaded.

The primary ingredients required are the theorem of minimum complementary energy and a stress function pertinent to a crack. The theorem states that, of all equilibrated stress fields which satisfy prescribed traction boundary conditions (here, the crack's flanks are stress free), the "actual" one is distinguished by a stationary (here, minimum) value of the complementary energy V*, where

$$V^* = \int_D W^*\left(\sigma_{ij}\right) dD - \int_{S_u} \tilde{u}_i t_i \, dS \tag{1}$$

In (1), integration proceeds over the domain D and that part S_u of its total boundary S where displacements are prescribed; $\tilde{u}_i$ are the prescribed displacements and t_i the corresponding tractions, σ_{ij} is the stress tensor, and W* is the complementary energy density given by

$$W^*\left(\sigma_{ij}\right) = \left[-\nu\left(\sigma_{kk}\right)^2 + (1+\nu)\sigma_{ij}\sigma_{ji}\right]/2E \tag{2}$$

[1]Carnegie-Mellon University, Pittsburgh, Pennsylvania, USA.
[2]Flight Dynamics Laboratory, Wright-Patterson Air Force Base, Ohio, USA.

for isotropic, Hookean material. (The usual indicial conventions are employed.) Anisotropic, elastic material is treated by suitable alteration of (2) and (3), below. While a fuller account of this theorem may be found in a good text, e.g., [1], our purpose is satisfied by the variational requirement $\delta V^* = 0$.

The appropriate stress function for isotropic planar bodies is due to Williams [2] and is written as

$$\begin{aligned}\chi(r,\theta) = \sum_{m=1}\Big\{&(-1)^{m-1}a_{2m-1}r^{m+1/2}\Big[-\cos(m-3/2)\theta + \frac{m-3/2}{m+1/2}\cos(m+1/2)\theta\Big]\\ &+ (-1)^{m-1}b_{2m-1}r^{m+1/2}[\sin(m-3/2)\theta - \sin(m+1/2)\theta]\\ &+ (-1)^{m}a_{2m}r^{m+1}[-\cos(m-1)\theta + \cos(m+1)\theta]\\ &+ (-1)^{m}b_{2m}r^{m+1}\Big[-\sin(m-1)\theta + \frac{m-1}{m+1}\sin(m+1)\theta\Big]\Big\}\end{aligned} \tag{3}$$

where (r,θ) are coordinates centred at the crack's tip in the usual manner. $\chi(r,\theta)$ satisfies equilibrium by definition and the traction conditions on the crack's flanks by construction. The stresses are

$$\begin{aligned}&\sigma_{11} \to \sigma_r = (1/r)\chi_{,r} + (1/r^2)\chi_{,\theta\theta} \qquad \sigma_{22} \to \sigma_\theta = \chi_{,rr}\\ &\sigma_{12} \to \tau_{r\theta} = -\Big[(1/r)\chi_{,\theta}\Big]_{,r} \qquad \sigma_{23} \to \tau_{\theta z} = 0\\ &\sigma_{13} \to \tau_{rz} = 0 \qquad \sigma_{33} \to \sigma_z\end{aligned} \tag{4}$$

and σ_z is either null or given by $\nu(\sigma_r + \sigma_\theta)$ in isotropic plane stress or plane strain, respectively. The stresses of interest are assembled in the form

$$\begin{Bmatrix}\sigma_r\\ \sigma_\theta\\ \tau_{r\theta}\end{Bmatrix} = \{\sigma\} = [S(r,\theta)]\{a\}$$

where [S] is a matrix whose entries depend solely on position as found by inserting (3) into (4), and

$$\{a\}^T = \left\{a_1 b_1 a_2 b_2 a_3 b_3 a_4 b_4 \ldots a_{2m-1} b_{2m-1} a_{2m} b_{2m}\right\}$$

Thus the entries in {a} appear in sets of four so that truncation of (3) at m = M gives 4M coefficients to be found.

Using G for the shear modulus and κ for the usual function of Poisson's ratio in planar isotropic elasticity, the compliance matrix [C] is written

$$8G[C] = \begin{bmatrix}\kappa+1 & \kappa-3 & 0\\ \kappa-3 & \kappa+1 & 0\\ 0 & 0 & 8\end{bmatrix}$$

and (2) is put into the familiar quadratic form

$$W^* = (1/2)\{a\}^T[S]^T[C][S]\{a\}$$

Typically, the displacement data $\tilde{u}_i$ will be resolved in orthogonal directions pertinent to the overall structure, or to the crack's position. Tractions t_i must be resolved in the same manner as $\tilde{u}_i$. Denoting these directions as (ξ,η) we write

$$\begin{Bmatrix}t_\xi\\ t_\eta\end{Bmatrix} = \{t\} = \Big[T(r,\theta)\Big|_{S_u}\Big]\{a\} \text{ and } \begin{Bmatrix}\tilde{u}_\xi\\ \tilde{u}_\eta\end{Bmatrix} = \{\tilde{u}\}$$

Note that {t} is computed from (3) and (4) via Cauchy's formula and, perhaps, Mohr's circle, and that [T] is evaluated along S_u only.

With the foregoing representations (1) becomes

$$V^* = (1/2)\{a\}^T[X]\{a\} - \{Y\}^T\{a\} \tag{5}$$

in which

$$[X] = \int_D [S]^T[C][S]dD, \quad \{Y\}^T = \int_{S_u}\{\tilde{u}\}^T[T]dS \tag{6}$$

Minimization of V^* leads to

$$[X]\{a\} = \{Y\} \tag{7}$$

as the algebraic problem statement†. Note that the problem's size is 4M irrespective of the number of data points on S_u. We must, however, carry through the quadratures in (6).

Code for this purpose has been devised. For a number of test problems considered, it was observed that $\{\tilde{u}\}$ does not vary rapidly along S_u but that the entries in [T] can. Hence a limited amount of data in $\{\tilde{u}\}$ is interpolated so that {Y} is determined by a large number of points using Simpson's one-third rule. To determine [X], however, a more elaborate tactic is needed. The interval $-\pi < \theta < \pi$ is divided into a dozen sectors, and Gaussian quadrature (using ten points radially and circumferentially) is employed in each sector. Size of the sectors is not necessarily uniform; we have dealt with rectangular paths S_u and let the corners and mid-points determine actual positions, as in Figure 1.

Accuracy of the quadrature used to find {Y} is essential so that any rigid motion in $\{\tilde{u}\}$ does not affect the result. We have observed that, by adding an arbitrary (and large) rigid motion to a given set of "active"

†This is the complement to the approach outlined in [3] for which traction boundary conditions on S are appropriate.

data $\{\tilde{u}\}$, a small change in $\{Y\}$ could be produced. For this reason, an intuitive scheme has been devised whereby this effect is made negligible. Letting $\xi = r \cos\theta$, $\eta = r \sin\theta$, we construct a new set of displacements,

$$\tilde{u}'_\xi = \tilde{u}_\xi + u_o - \omega\eta$$

$$\tilde{u}'_\eta = \tilde{u}_\eta + v_o + \omega\xi$$

and the quantity

$$\tilde{v}' = -\tilde{u}'_\xi \sin\theta + \tilde{u}'_\eta \cos\theta$$

$$= \tilde{v} - u_o \sin\theta + v_o \cos\theta + \omega r$$

Summing the data along S_u and setting $\Sigma\tilde{u}_\xi = \Sigma\tilde{u}_\eta = \Sigma\tilde{v} = 0$ to approximate the notion of no crack-tip movement gives three equations whose solution is an estimate of u_o, v_o, and ω. The original $\{\tilde{u}\}$ is then recovered. It was found that, where rigid motion is large relative to the active displacements, this scheme virtually negates the rigid motion. For rigid motion of the same magnitude as the active displacements, however, the scheme loses some accuracy. Owing to the care involved in quadrature along S_u, the net effect is negligible in terms of the solution $\{a\}$. Hence, while we cannot rigorously account for rigid motion, we have found means for negating its influence.

Some of our test problems give a sense of performance. We have determined, first, that S_u is best taken as approximately equilateral and, second, that the crack's tip should be near the middle of the domain. Under these conditions, two additional test problems were solved. In the first, S_u was rectangular and oriented such that its edges were parallel and normal to the crack's plane; $\{\tilde{u}\}$ was determined by computing displacements from the series [3], having assumed that

$$a_i = -1.0 \times 10^{1-i} \quad i = 1,8 \tag{8}$$

and that all other coefficients are null. In the second problem, a similar path S_u was rotated clockwise 45 deg and the non-zero coefficients were taken to be

$$a_i = -1.0 \times 10^{1-i} \quad b_i = 1.0 \times 10^{1-i} \quad i = 1,8 \tag{9}$$

(except that† $b_2 = 0$), to obtain a more complicated set of displacements. Using these two data sets at 121 points along S_u, as input, solutions to (7) were obtained as shown in Tables 1 and 2. These coefficients were then used to compute displacements and stresses on S_u; agreement with values derived from (8) and (9) was within 0.013 percent of their respective maximum values.

†Close examination of the b_2 term in (1) shows that it does not affect stress. In fact, b_2 is proportional to a rigid rotation, just as a_o and b_o - were they to appear - denote rigid translations. The code automatically sets b_2 to zero.

Other problems used to test the procedure were taken from earlier finite element results (in the elastic range) where stress intensity was known to within a few percent. That is, although highly reliable displacement data could be obtained, there is a modest uncertainty in the value of stress intensity based on the finite element data itself. Nonetheless the present method determined values of stress intensity within the uncertainty band (nominally 5 percent). It should be noted, however, that we found it advisable to interpolate the initial values of $\{\tilde{u}\}$ to provide data at 120 to 160 nearly equispaced points on S_u, and that $M = 7$ was required to achieve this result. The associated CPU time (1108, Exec 2) was about twenty seconds per case, with only modest storage requirements. Thus the procedure appears to be workable and to meet the needs stated at the outset. Moreover, this procedure provides vastly more resolution in the stress and displacement variation near the crack's tip than is usually obtained from finite element analyses.

With this procedure in hand, it is useful to employ speckle photography to measure the displacement data $\{\tilde{u}\}$. This procedure has been developed [4,5] specifically to make *in situ* observations and may briefly be outlined. The diffuse surface of an object and its associated speckle pattern caused by the illuminating laser is imaged onto a sensitized film plate. The result is a recording of a random variation of bright and dark spots whose size depend upon the characteristics of the optical recording system and are usually on the order of a thousand spots per millimeter. If the object is deformed, a new random variation can be recorded which, if superimposed upon the variation corresponding to the undeformed condition will result in a set of "speckle pairs" that can be related to the vector displacement field describing the deformation. If an unexpanded beam from a laser is passed through the developed image in the plate, a circular halo of light with a pattern of parallel fringes similar to Young's Fringes is observed. The distance between these fringes can be related to the displacement which occurred on the test specimen. By moving the laser beam around the image, a displacement field can be calculated.

At this point, the coupling of the two techniques is in progress, and additional results should be reported soon. It is clear from preliminary work, however, that the effort is highly interactive: refinement of the computational procedure has been stimulated by the character of actual displacement data, and the orientation and shape of the path followed by the interrogating laser have been adjusted to meet computational requirements. On this basis an overall procedure for extracting stress intensity value(s) from *in situ* observations is established.

ACKNOWLEDGEMENT

This work is proceeding with the support of the United States Air Force Flight Dynamics Laboratory and Carnegie-Mellon University, for which we are grateful.

REFERENCES

1. FUNG, Y. C., "Foundations of Solid Mechanics", Prentice-Hall, Englewood Cliffs, 1965, Chapter 10.
2. WILLIAMS, M. L., Journal of Applied Mechanics, 24, 1957, 109-114.

3. EWING, P. D., SWEDLOW, J. L. and WILLIAMS, J. G., International Journal of Fracture, 12, 1976, 85-93.
4. ADAMS, F. D. and MADDUX, G. E., "On Speckle Diffraction Interferometry for Measuring Whole Field Displacements and Strains", AFFDL TR-73-123.
5. ADAMS, F. D. and MADDUX, G. E., "Dual Plate Speckle Photography", AFFDL TR-75-57-FBR.

Table 1 Known Coefficients and Computed Values

i	a_i (known)	a_i (computed)	b_i (known)	b_i (computed)
1	-1.0	-0.99999422	0.0	0.00000002
2	-0.1	-0.10004858	0.0	0.0
3	-0.01	-0.00995341	0.0	0.00000010
4	-0.001	-0.00100015	0.0	0.00000005
5	-0.0001	-0.00009944	0.0	0.00000014
6	-0.00001	-0.00001922	0.0	-0.00000019
7	-0.000001	0.00000893	0.0	-0.00000005
8	-0.0000001	0.00000250	0.0	0.00000001

Table 2 Known Coefficients and Computed Values (Crack at 45 Deg)

i	a_i (known)	a_i (computed)	b_i (known)	b_i (computed)
1	-1.0	-0.99998467	1.0	0.99999324
2	-0.1	-0.10008076	0.0	0.0
3	-0.01	-0.00987082	0.01	0.00999148
4	-0.001	-0.00098246	0.001	0.00100222
5	-0.0001	-0.00004756	0.0001	-0.00008448
6	-0.00001	0.00003787	0.00001	-0.00001321
7	-0.000001	-0.00003930	0.000001	-0.00002506
8	-0.0000001	-0.00000196	0.0000001	0.00002333

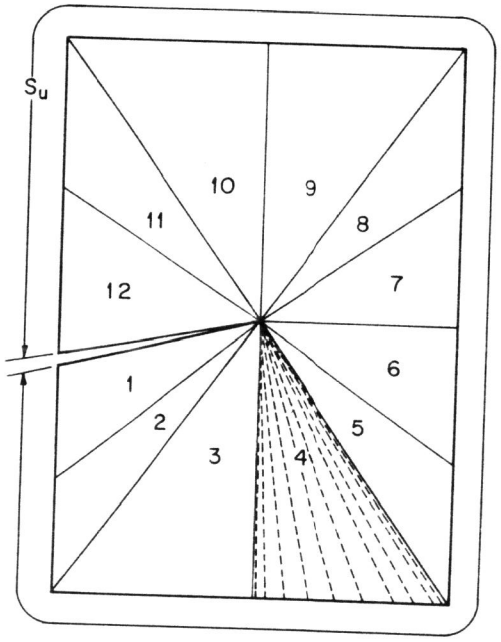

Figure 1 Geometry, Showing Data Path S_u and Interior Quadrature Regions